Decomposition of lanthanum hafnate at high pressures

Nandini Garg,[1,*] K. K. Pandey,[1] Chitra Murli,[1] K. V. Shanavas,[1] Balaji P. Mandal,[2] A. K. Tyagi,[2] and Surinder M. Sharma[1]
[1]*High Pressure Physics Division, Bhabha Atomic Research Center, Trombay, Mumbai 400085, India*
[2]*Chemistry Division, Bhabha Atomic Research Center, Trombay, Mumbai 400085, India*
(Received 11 January 2008; published 13 June 2008)

Our high pressure x-ray diffraction and Raman scattering studies on lanthanum hafnate ($La_2Hf_2O_7$) establish that it decomposes into its constituent oxides beyond ~18 GPa. These results are supported by our first-principles total energy calculations. Raman scattering results also imply that the products of dissociation are in an amorphouslike state beyond 50 GPa but crystallize slowly upon release of pressure.

DOI: 10.1103/PhysRevB.77.214105 PACS number(s): 61.50.Ks, 61.05.cp, 78.30.−j, 71.15.Mb

I. INTRODUCTION

$A_2B_2O_7$ compounds having pyrochlore structure are employed for a wide range of applications such as in catalysis,[1] dielectrics,[2] thermal barrier coatings,[3] fuel cells,[4] etc. In addition, due to the structural compatibility with several radionuclides, these pyrochlores have also been perceived as materials for encapsulation of actinide rich nuclear waste.[5–13] Recently, some of the rare-earth pyrochlores have also been shown to exhibit spin-ice and spin-liquid behavior.[14]

Since several A^{3+} and B^{4+} cations have suitable ionic radii $[1.8 \geq (r_a/r_b) \geq 1.46]$ for the formation of the pyrochlore structure,[15] a large number of pyrochlore oxides known in the nature are of the $(3^+,4^+)$ type, i.e., $A_2^{3+}B_2^{4+}O_7$. The radius ratio for lanthanum hafnate is ~1.6 and hence it crystallizes in the pyrochlore structure.[15] The pyrochlore structure belongs to $Fd\bar{3}m$ space group (fcc) with A^{3+} cations occupying the 16d, B^{4+} atoms at 16c and oxygen occupying 48f and 8b positions, respectively (setting 2). As all other atoms occupy special crystallographic sites, the only internal positional parameter that can vary is "x" of 48f oxygen atoms. The structure can be viewed as made of eightfold and sixfold coordination polyhedra of oxygen atoms around A and B cations (Fig. 1) and these polyhedra change shape with the value of x parameter. For pyrochlore structure x lies in the range 0.3125–0.375, and for $x \geq 0.375$ the structure becomes defect fluorite.[15]

It has been observed that substitution of the B cations with larger and larger ions progressively increases disorder.[16] Ion irradiation[17–19] also introduces disorder including even eventual amorphization under heavy dosage.[20] It is well known that in many compounds, particularly having polyhedral network structures, amorphization can also be induced by subjecting the compounds to high pressure.[21–25] In all the cases of pressure induced amorphization, the amorphous state is a kinetically preferred state. The onset pressure for many of these is determined by the limiting distances of nonbonded atoms.[25] In some such cases, the inaccessible high-pressure equilibrium phase could be the products of the dissociation.[25] Recent studies on pyrochlores have shown that many of these amorphize at high pressures either directly or after a precursor crystal to crystal phase transition.[26–29] Zhang *et al.* have shown that samarium titanate amorphizes at 51 GPa[26,27] and have suggested that the disorder observed at ~40 GPa may be due to the random orientations of TiO_6 octahedra and not due to the disordering of Sm^{3+} ions. However, gadolinium titanate has been shown to undergo a subtle isostructural phase transition at ~9 GPa.[28] There are mixed reports about the high-pressure behavior of $Tb_2Ti_2O_7$, as Apetrei *et al.*[30] have reported that this compound is stable up to 42 GPa whereas Kumar *et al.*[31] showed that it transforms to a monoclinic structure at 40 GPa, before becoming amorphous at higher pressures. Recent studies on cadmium niobate[32] have shown appearance of a small amount of metallic cadmium at ~4 GPa followed by structural phase transitions to defect fluorite, monoclinic or orthorhombic phase which, when quenched from ~28 GPa, transforms to a mixture of phases, including amorphous phase.

So as to further understand the nature of pressure induced changes occurring in this class of compounds, we have now carried out detailed studies on $La_2Hf_2O_7$ (LH) using x-ray diffraction, Raman spectroscopy, and the first-principles calculations.

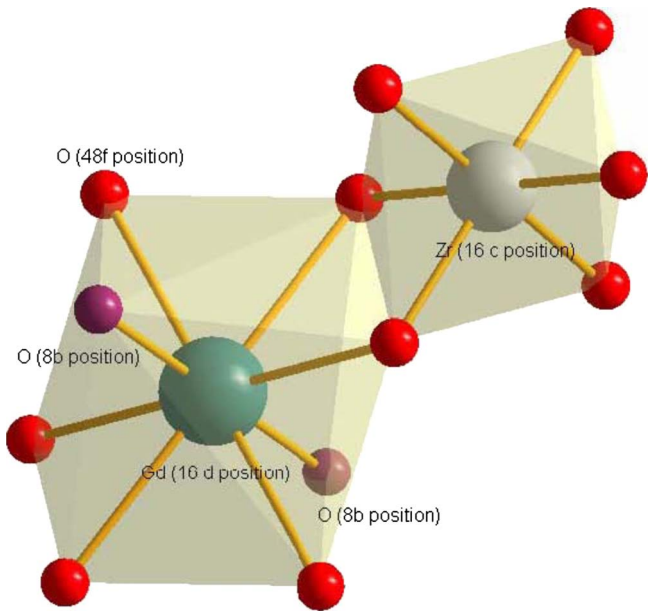

FIG. 1. (Color online) The coordination of the A^{3+} (La) and B^{4+} (Hf) atoms with oxygen atoms in a pyrochlore structure.

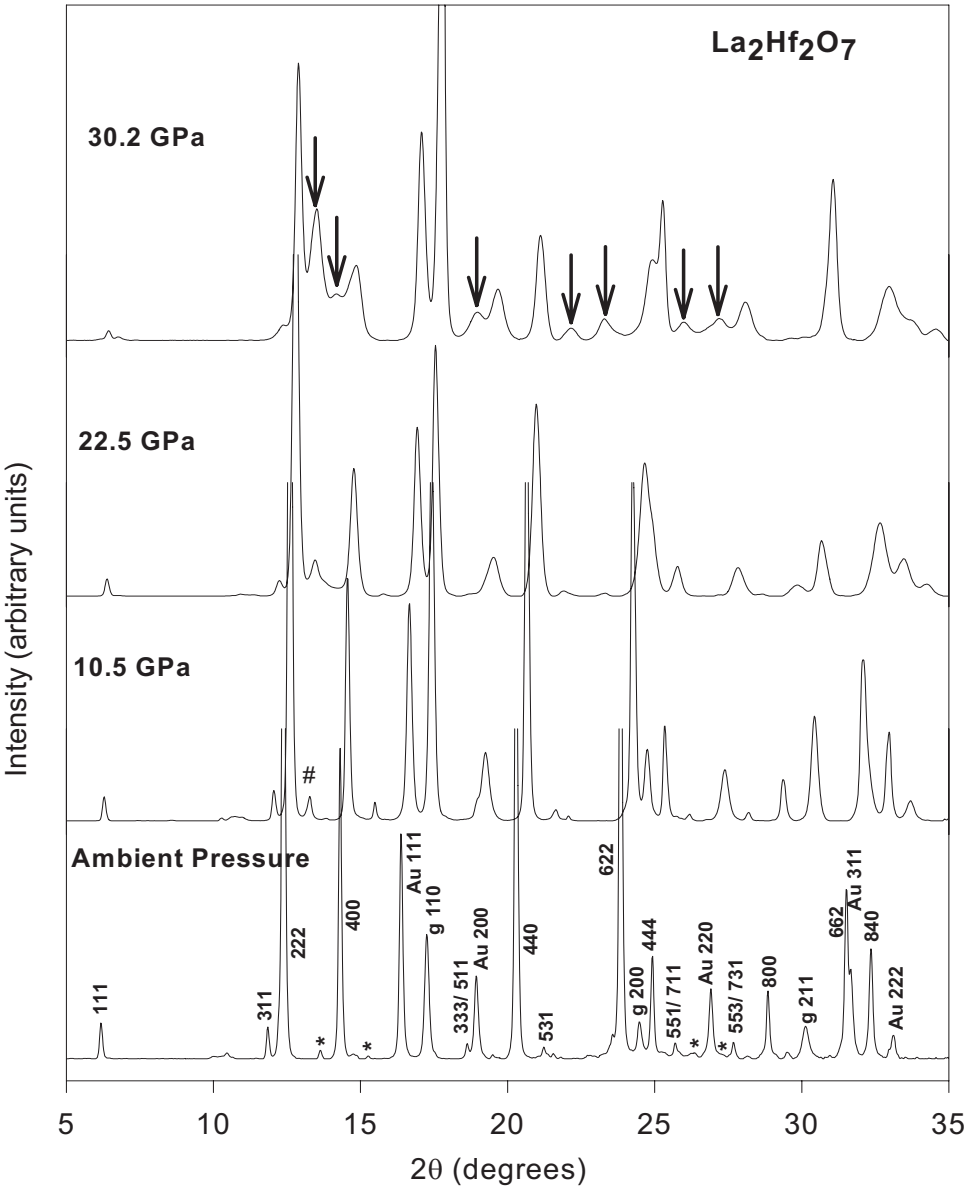

FIG. 2. The diffraction patterns of lanthanum hafnate at different pressures. The indices of the sample peaks are shown at the ambient conditions. The diffraction peaks from the gasket are marked as "*g*" and those of the pressure marker are marked as 'Au' respectively. The star (∗) indicates the diffraction peaks of hafnium oxide (monoclinic phase). The # indicates the most intense peak (211) of hafnium oxide (orthorhombic phase I) and the arrows indicate the new diffraction peaks, identifiable with those of the dissociation products.

II. EXPERIMENTAL DETAILS

Lanthanum hafnate was prepared in our laboratory through the standard solid state route. To remove the moisture and other volatile impurities, analytical reagent (AR) grade La_2O_3 and HfO_2 were first heated at 1173 K for about 12 h. Stoichiometric amounts of the reactants were weighed to get the composition $La_2Hf_2O_7$. Well ground mixtures were heated in the pellet form at 1473 K for 36 h. After this, the materials were reground, repelletized and heated at 1573 K for 36 h. In order to attain a better homogeneity, the products obtained after second heating were again ground, pelletized and heated at 1673 K for 48 h, which was the final annealing temperature of all the specimens. The heating and cooling were carried out at a rate of 2 K/min in a static air environment.

The compound thus formed was characterized with the help of x-ray diffraction and Raman spectroscopy. The cell constant of lanthanum hafnate was found to be 10.78 ± 0.01 Å, which is in good agreement with the earlier reported value of 10.78 Å.[15] At ambient conditions, we observed a few diffraction peaks which could be ascribed to the impurity constituent oxide i.e., hafnium oxide (shown by "∗" in Fig. 2) and the Rietveld analysis of our recorded diffraction pattern gives its abundance to be ~1%.

For x-ray diffraction experiments the powder samples of lanthanum hafnate along with a few particles of gold (pressure markers) were loaded into a 100 μm hole of a preindented tungsten gasket (~70 μm) in a diamond anvil cell. 4:1 methanol-ethanol mixture was used as a pressure transmitting medium and the pressure was determined from the

known equation of state (EOS) of gold.[33] These experiments were carried out at the XRD1 beamline of the Elettra synchrotron source using the x-rays of wavelength 0.67 Å. The two-dimensional diffraction rings were converted to one-dimensional diffraction patterns using the FIT2D software.[34] The cell constants were determined by the Le Bail method using the GSAS software.[35] The high-pressure experiments were carried out up to 30 GPa.

For Raman measurements a single speck of a polycrystalline sample of lanthanum hafnate was loaded in a 50 μm hole of a preindented tungsten gasket (~30 μm) in a diamond anvil cell. In this case also we used 4:1 methanol-ethanol mixture as a pressure transmitting medium but the pressure was determined from the well known ruby fluorescence method.[36] High-pressure Raman experiments were carried out up to ~65 GPa using our indigenous micro Raman system. In this instrument, we have used a 20× objective with a confocal optics and a CCD based single stage spectrograph along with a super notch filter. For the measurements presented here we used 532 nm line of solid state diode laser as the excitation source. A laser spot of size less than 10 μm could be focused on the desired portion of the sample inside the gasket hole with the help of a viewing system. This helps to reduce the background noise contributed by the diamond and gasket substantially.

III. RESULTS AND DISCUSSION

A. X-ray diffraction experiments

The diffraction patterns of lanthanum hafnate at a few representative pressures are shown in Fig. 2. It was observed that at ~6.5 GPa a new diffraction peak (shown by "#" in Fig. 2) started emerging at $2\theta \sim 12.8°$ and the intensity of the (111) peak of hafnium oxide (at $2\theta \sim 13.8°$) started diminishing. Le Bail analysis of the diffraction pattern indicated that this new diffraction peak may be from the high-pressure orthorhombic phase (I) of hafnium oxide. (It is the strongest (211) diffraction peak of this phase). Upon increase of pressure beyond 18 GPa, the appearance of new diffraction peaks (marked with arrows in Fig. 2) and diminishing intensities of the diffraction peaks of the initial cubic phase are indicative of a structural change in this compound.

The experimentally determined pressure-volume behavior of lanthanum hafnate is shown in Fig. 3. Within the experimental certainty, no unusual changes in the P-V behavior, ascribable to structural changes, could be observed. The pressure-volume data were fitted with the third order Birch–Murnaghan equation of state[37] with the help of the EOSFIT.[38] The fits gave $K_o = 147.2$ GPa, $K' = 7.9$. Our equation of state studies on some other IVB pyrochlores compounds like $Sm_2Ti_2O_7$ and $Gd_2Zr_2O_7$ had given $K_o = 173.2$ GPa, $K' = 9.25$, $K_o = 153.4$ GPa, and $K' = 10.5$, respectively,[39] indicating that these compounds are fairly incompressible. These values of the bulk moduli support the conclusions derived by Panero *et al.* about the variation of B with unit cell volume.[40] Relatively larger values of K′ for these compounds are somewhat similar to the results of recent studies on $ZrSiO_4$ ($K = 225$ GPa) which has $K' = 6.5$.[41] Constraining K′ to 4 results in poorer fits, but gives higher bulk moduli for all the compounds mentioned above and, in particular, for lanthanum hafnate it is 187 GPa.

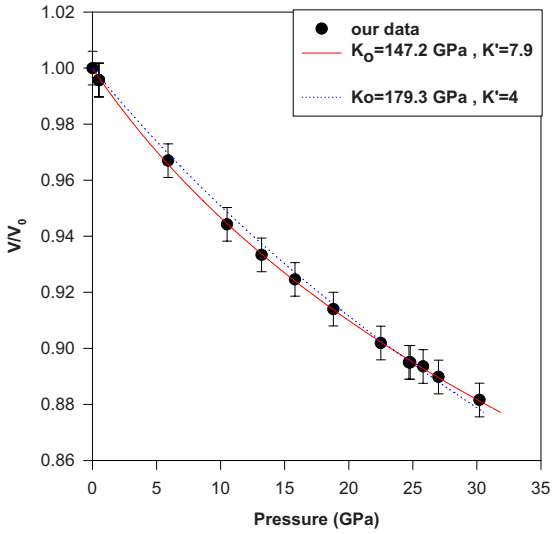

FIG. 3. (Color online) V/V_o of Lanthanum hafnate as a function of pressure. The red solid line shows the fit to the third order Birch–Murnaghan equation of state. The blue dashed line shows the fit to the second order BM equation of state i.e., $K' = 4$.

At ~18 GPa, in addition to the new diffraction peaks, the diffraction pattern of lanthanum hafnate had all the diffraction peaks of the initial cubic phase, implying the coexistence of the new and the parent phases. The structure of the new phase was neither similar to that of the high-pressure fluorite structure (since the characteristic (002) and (022) diffraction peaks of the fluorite structure were not observed) nor belonged to the Pc and C2 monoclinic space groups, i.e., the predicted high-pressure phases of the terbium stannate. We extended the search of structure through group-subgroup analysis as implemented in Powder Cell for Windows (PCW) software.[42] However, none of the structures corresponding to the subgroups were able to provide a good fit to the diffraction data. A preliminary analysis of the diffraction data seemed to indicate that the high-pressure diffraction pattern could be a mixture of the constituent oxides. Hence to determine whether the new diffraction peaks were indeed arising due to the constituent oxides we carried out a Rietveld analysis with the help of the GSAS software.[35] The refinement was carried out based on five phases: cubic lanthanum hafnate, the denser oxides of hafnium and lanthanum, gold (pressure marker) and tungsten (gasket). The goodness of fit parameters at 18 GPa and 26 GPa are $R_{wp} = 0.048, 0.04$; $R(F^2) = 0.099, 0.12$, respectively. The Rietveld fit at 26 GPa is shown in Fig. 4. Our refinement results indicate that the structure of lanthanum oxide is similar to its ambient pressure structure whereas the structure of hafnium oxide is similar to the high-pressure orthorhombic-II phase (Cotunnite phase).[43] Relevant structural parameters of these phases are given in Table I. The weight fraction of lanthanum hafnate, as estimated from Rietveld analysis, decreases approximately[44] from 56% to 21% whereas the abundances of oxides increases from 17% to 42%, when the pressure is raised from 18 GPa to 30 GPa. The goodness of fit parameters as well as the increasing fraction of the constituent

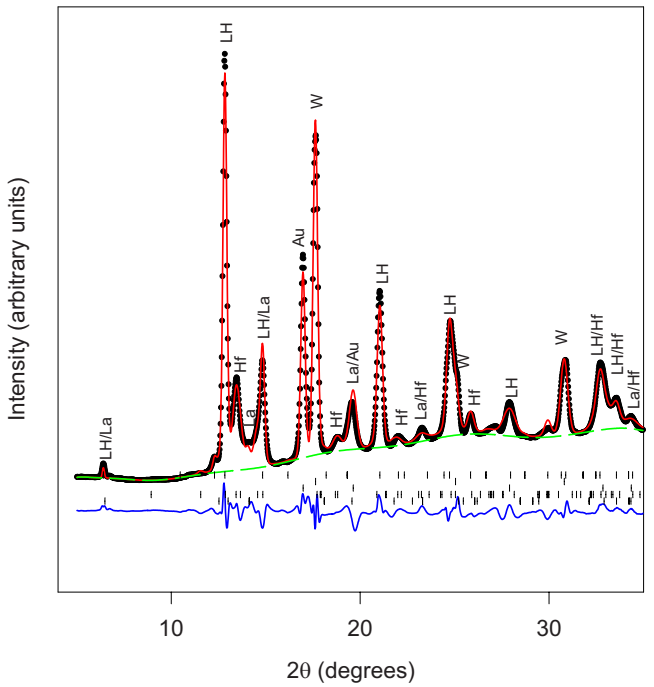

FIG. 4. (Color online) Rietveld fits to the recorded diffraction pattern at 26 GPa (red). The green dashed line shows the subtracted background and vertical bars give the expected positions of the diffraction peaks from the sample (LH), the gasket (w) and the pressure marker (Au). The difference in the calculated and experimental diffraction pattern is given at the bottom of the graph (blue). The diffraction peaks from lanthanum hafnate, hafnium oxide (orthorhombic-II) and lanthanum oxide, gold and tungsten are marked as LH, Hf, La, Au, and W, respectively.

oxides strongly suggest the possibility that lanthanum hafnate disassociates at high pressures.

As mentioned earlier the pyrochlore structure of lanthanum hafnate coexists with the new phase up to the highest measured pressure of 30 GPa. As mentioned above, structural refinement of lanthanum hafnate in the pyrochlore phase requires only the refinement of $x-O_{48f}$ parameter which is shown in Fig. 5. These results show that x-parameter starts increasing beyond 18 GPa and around 30 GPa it is very close to the limit of stability of the pyrochlore structure, as discussed above. Our refinement suggests that the remnant pyrochlore structure may transform into the defect fluorite structure at still higher pressures, as also observed in cadmium niobate.[32] However, since the Raman spectra give a better indication of the fluorite structure, we carried out Raman scattering studies also on lanthanum hafnate.

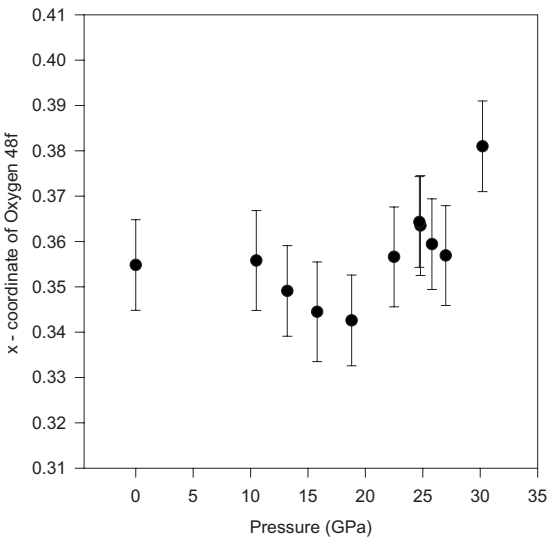

FIG. 5. The variation of the "x" parameter of the 48f oxygen for $La_2Hf_2O_7$, as a function of pressure.

B. Raman measurements

The Raman spectra of the pyrochlore structure have six Raman active modes, which according to group theoretical analysis[45] are $\Gamma=A_{1g}+E_g+4F_{2g}$. At ambient conditions the modes at 320, 338, 417, 514, and 538 cm^{-1} [Fig. 6(a)] could be assigned to F_{2g}, E_g, F_{2g}, A_{1g} and F_{2g}, respectively, and the broad band at 767 cm^{-1}, which was also observed by Vandenborre *et al.*, could be due to the distortion of the hafnate octahedra.[46]

The broadening and reduction in intensities of the Raman modes beyond 18 GPa indicate that the initial sample of

TABLE I. Structural parameters of the daughter products at 30 GPa.

Hafnium oxide (Pnma) (30 GPa)						
Cell constants (Å)	5.6268	3.351	6.612	90°	90°	90°
Fractional coordinates	Hf	0.2462	0.25	0.1125		
	O1	0.345	0.25	0.446		
	O2	0.022	0.75	0.3398		
Space group no.	62					
Lanthanum oxide ($P\bar{3}2/m1$) (30 GPa)						
Cell constants (Å)	3.54	3.54	5.91	90°	90°	120°
Fractional coordinates	La	0.3333	0.66666	0.2		
	O1	0.33333	0.66666	0.645		
	O2	0.000	0.000	0.000		
Space group no.	164					

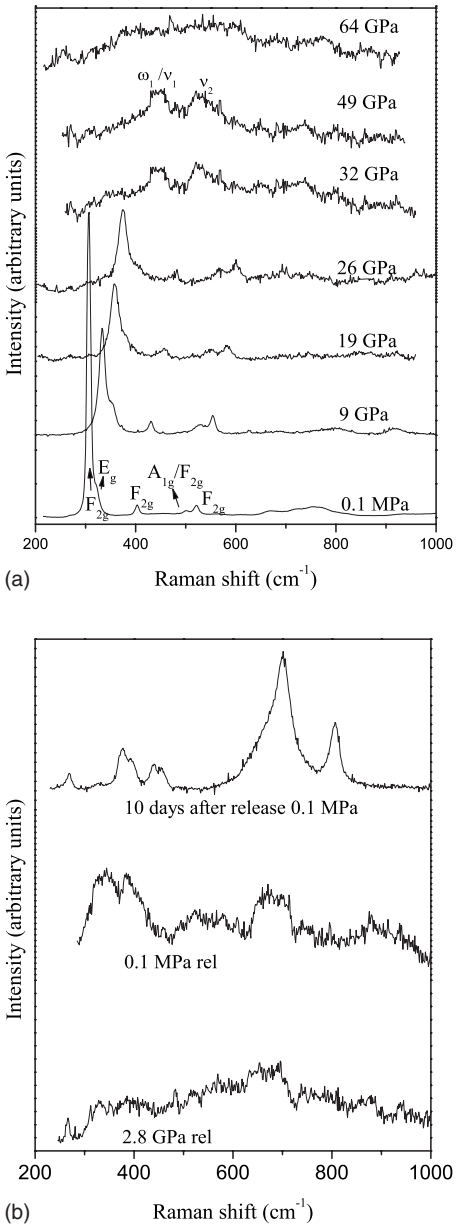

FIG. 6. Raman scattering data of lanthanum hafnate at different pressures (a) increasing pressure. The Raman modes of lanthanum hafnate are shown in the ambient pressure run. The new modes at 49 GPa are (ω_1) from La_2O_3 and (υ_1, υ_2) from HfO_2. (b) Decreasing pressure.

lanthanum hafnate has undergone some significant changes. The broadening of the Raman modes continued up to 30 GPa and beyond this pressure, these Raman modes were replaced by new Raman bands at 445 and 525 cm^{-1}. Our results suggest that the structural transformation which was initiated at ~18 GPa was complete only beyond 30 GPa.

The Raman spectrum of fluorites has a single broad band as the seven oxygen ions in this structure are randomly distributed over the eight anion sites, essentially giving rise to disorder. In fact, the existence of anionic disorder helps stabilization of the defect fluorite structure, as shown by Glerup *et al.*[16] for $Y_2Ti_{2-y}Zr_yO_7$.[47] However, we did not observe a single broad band beyond 30 GPa. Instead, two new modes were observed at 445 and 525 cm^{-1} overlying a broad background. Comparison with earlier[48] Raman spectroscopic studies on hafnium oxide strongly suggests that these new Raman modes may belong to the Raman modes of orthorhombic-II phase of hafnium oxide. However, in our spectra these modes are not as well resolved as those observed by Jayaraman *et al.*[48] As the strongest Raman modes of the high-pressure phase of hafnium oxide are more intense than the broad Raman band of fluorite, they are easily discernible over the large broad band of the fluorite phase. Our high-pressure Raman studies on lanthanum oxide indicate that it does not undergo any phase transition up to ~26 GPa. The Raman band of lanthanum oxide also falls close to 430 cm^{-1} and could be coinciding with the Raman band of HfO_2. These results suggest that lanthanum hafnate starts disassociating into its constituent oxides beyond 18 GPa and the remnant pyrochlores may be transforming into the fluorite structure beyond 30 GPa.

Upon further increasing the pressure up to 65 GPa the Raman modes became very broad indicating that the mixture of new disassociated phases may have transformed to an amorphous state. The Raman spectra recorded immediately after the release of pressure was also found to be very broad, suggesting the retention of the disordered state upon release of pressure [Fig. 6(b)]. However, the emergence of new Raman modes at 269, 377, 393, 440, 455, 702, and 807 cm^{-1} in the spectra recorded after ~10 days of release of pressure, suggests a sluggish transformation of the disordered state to some new ordered phases. These new modes are quite similar to the Raman modes of tetragonal HfO_2 and ZrO_2 quenched from 51 and 60 GPa, respectively.[48,49] The mode at ~800 cm^{-1} is quite strong while the other modes at lower frequencies are weak. This mode may be of the disordered HfO_6 octahedra, as mentioned earlier. A similar broad mode was observed in samarium titanate ~40 GPa and was attributed to the breathing mode of the randomly oriented TiO_6 octahedra.[26]

C. First-principles total energy calculations on lanthanum hafnate and its daughter products

To provide further support for the conclusions derived from our experimental results, we have carried out total energy calculations. These first-principles density functional theory (DFT) calculations were performed within the generalized gradient approximation (GGA) (Ref. 50) using projector augmented wave (PAW) method[51,52] as implemented in the Vienna *Ab Initio* Simulation Package (VASP).[53,54] Simulations were performed by explicitly treating 11 valence electrons for La($5s^25p^65d^16s^2$), 10 for Hf($5p^65d^26s^2$) and 6 for oxygen ($2s^22p^4$). Brillouin-zone integrations are performed with a Gaussian broadening of 0.1 eV during all structural optimizations. A Monkhorst–Pack **k**-point mesh of $4\times4\times4$ and plane-wave cutoff of 600 eV were found to provide good convergence of the computed ground-state properties. Structural optimizations were continued until the forces on the atoms had converged to less than 1 meV/A and the pressure on the cell had minimized within the constraint of constant volume.

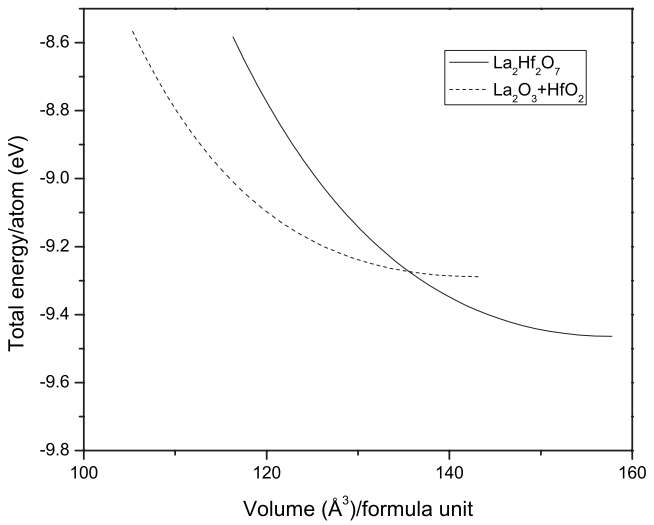

FIG. 7. Calculated total energy versus volume per formula unit for lanthanum hafnate and its disassociation products.

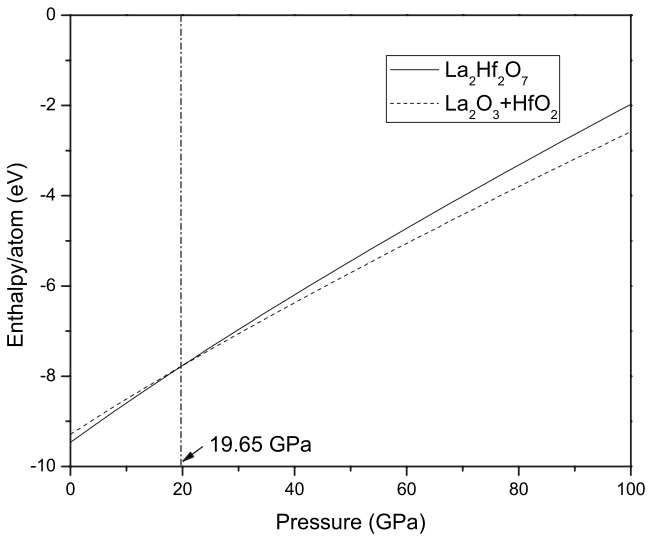

FIG. 8. Calculated enthalpy versus pressure for lanthanum hafnate and its disassociation products.

The initial structures used in these simulations were the same as determined from our x-ray diffraction studies mentioned above. The total energy $E(V)$ was calculated as a function of the volume, for each of the three phases viz., $La_2Hf_2O_7$, La_2O_3 and HfO_2 (monoclinic and orthorhombic (O-II), respectively). At each volume, the positional coordinates were optimized by structure relaxation and the structure with the lowest energy was obtained. At nonzero temperatures the stable structure corresponds to minimum Gibbs free energy (G=E+PV−TS). However, since these calculations were carried out at $T=0$ K the structural stability is related to enthalpy.

For comparison with total energy of $La_2Hf_2O_7$, the total energy and volume of the mixture of products of dissociation [i.e., $La_2O_3+HfO_2$ (O-II)] is calculated as

$$A_{\text{product}} = 2 \times A(\text{HfO}_2) + A(\text{La}_2\text{O}_3), \quad \text{where} \quad A = E \text{ or } V.$$

Figure 7 shows the total energy E as a function of volume (per formula unit of lanthanum hafnate) in the composite and disassociated phases. The solid and dashed lines are fits of the computed data of parent and daughter states to the Murnaghan equation of state given below:[55]

$$E(V) = E_0 + \frac{B_0 V}{B_0'}\left[\frac{(V_0/V)^{B_0'}}{B_0' - 1} + 1\right] - \frac{B_0 V_0}{B_0' - 1}, \qquad (1)$$

where E_0 is the minimum energy for the initial volume V_0. B_0 and $B_0'=4.1$ are the bulk modulus and pressure derivative of bulk modulus, respectively. The equation of state of lanthanum hafnate determined from these first-principles calculations when fitted to Birch–Murnaghan EOS gives $B_0'=165$ GPa, B_0', which is reasonably close to the experimental value. The sum of total energies of the disassociated products at zero pressure is higher than that of lanthanum hafnate by 175 meV. However, below a volume of 137 Å^3 the total energy of the disassociated phase is always lower than that of the parent phase.

The calculated enthalpy as a function of pressure is given in Fig. 8 which shows that beyond ~20 GPa the disassociation products are more stable than lanthanum hafnate. Thus the results of our first-principles calculations strongly support the conclusions deduced from our experimental measurements.

D. Discussion

Dissociation of a compound into a mixture of its constituents at elevated pressures is likely to be primarily controlled by the atomic diffusion which is generally high only at high temperatures. It is well known that even if the constituent daughter products have a lower total energy than the parent compound at high pressures, decomposition may not be realized, as the volume per formula unit of the daughter compounds may be larger than that in the parent compound. The existence of a potential barrier on the transformation path to the daughter phases/products would lead to kinetics frustration, eventually driving the system to an amorphous/disordered state.[25] However, in the present case the volume considerations are favorable for the decomposition. The volumes per formula unit of lanthanum hafnate, lanthanum oxide (LO) and hafnium oxide (HO) determined from our x-ray diffraction data at 18 GPa are 142.85, 64.25, and 30.96 A^3, respectively. Hence the fractional decrease in the volume upon decomposition is $[V_{\text{LH}}-(V_{\text{LO}}+2^*V_{\text{HO}})]/V_{\text{LH}}$, i.e., ~12%. In fact from the first-principles calculations also the computed volume drop at the transition pressure was determined to be 11%, which is in agreement with the experimentally observed value. Thus, higher density as well as lower enthalpy of the daughter products at high pressures favor decomposition in lanthanum hafnate.

In principle, it is possible that the existence of ~1% of high pressure polymorph of HfO_2 could act as a nucleation center and aid the decomposition. However, decomposition at high pressures has been observed earlier in scheelite structured lithium gadolinium fluoride[56] and a negative thermal

expansion material zirconium vandate.[57] It is interesting to note that in zirconium vandate samples, 1 to 2% unreacted constituent oxides existed, however, from the published data it is not possible to discern the presence of unreacted components in lithium gadolinium fluoride samples. Hence the evidence at this stage is inconclusive whether the decomposition at high pressures is aided by the presence of a nucleating component. Further experiments are needed to settle this issue unambiguously.

IV. CONCLUSIONS

In conclusion, our experimental observations, supported by our first-principles calculations, show that lanthanum hafnate disassociates into a mixture of HfO_2 and La_2O_3 beyond 18 GPa. These oxides are found to be disordered at 65 GPa and retain the disordered state upon immediate release of pressure. However, our results show that this retrieved amorphous state partially and slowly transforms to a mixture of crystalline forms of HfO_2 and La_2O_3. The results presented here are interesting in the sense that this is the first time that a pyrochlore has been shown to decompose under high pressures. Since lanthanum hafnate is one of potential compounds for use in the nuclear waste disposal, (due to the presence of Hf as a neutron absorber), present results may have implications on its utility in this context.

ACKNOWLEDGMENTS

We would like to thank E. Busetto and Maurizio Polentarutti for their help during the experiments at the XRD1 beamline at Elletra. We would also like to thank S. K. Sikka for his critical comments and useful suggestions.

*Corresponding author. FAX: +91-22-25505151; nandini@barc.gov.in

[1] Z. Jyh-Myng, A. S. Kumar, and C. Jyh-Cheng, J. Mol. Catal. A: Chem. **165**, 177 (2001).
[2] Juan C. Nino, Hyuk J. Youn, Michael T. Lanagan, and Clive A. Randall, J. Mater. Res. **17**, 1178 (2002).
[3] M. M. Gentleman and D. R. Clarke, Surf. Coat. Technol. **200**, 1264 (2005).
[4] Zhimin Zhong, Electrochem. Solid-State Lett. **9**, A215 (2006).
[5] G. R. Lumpkin, K. P. Hart, P. J. McGlinn, and T. E. Payne, Radiochim. Acta **66/67**, 469 (1994).
[6] K. E. Sickafus, L. Minervini, R. W. Grimes, J. A. Valdez, M. Ishimaru, F. Li, K. J. McClellan, and T. Hartmann, Science **289**, 748 (2000).
[7] A. E. Ringwood, S. Kesson, N. G. Ware, W. Hibberson, and A. Major, Nature (London) **278**, 219 (1979).
[8] R. C. Ewing, W. J. Weber, and J. Lian, J. Appl. Phys. **95**, 5949 (2004).
[9] S. X. Wang, L. M. Wang, R. C. Ewing, and K. V. G. Kutty, *Microstructural Processes in Irradiated Materials*, MRS Symposia Proceedings No. 540 (Materials Research Society, Pittsburgh, 1999), p. 355.
[10] A. A. Digeos, J. A. Valdez, K. E. Sickafus, S. Atiq, R. W. Grimes, and A. R. Boccaccini, J. Mater. Sci. **38**, 1597 (2003).
[11] S. X. Wang, B. D. Begg, L. M. Wang, R. C. Ewing, W. J. Weber, and K. V. G. Kutty, J. Mater. Res. **14**, 4470 (1999).
[12] K. V. Govindam Kutty, E. Asuvathraman, R. R. Madhavan, and Hrudananda Jena, J. Phys. Chem. Solids **66**, 596 (2005).
[13] John E. Greedan, Chem. Mater. **10**, 3058 (1998).
[14] I. Mirebeau, I. N. Goncharenko, P. Cadavez-Peres, S. T. Bramwell, M. J. P. Gingras, and J. S. Gardner, Nature (London) **420**, 54 (2002).
[15] M. A. Subramanian, G. Aravamudan, and G. V. Subba Rao, Prog. Solid State Chem. **15**, 55 (1983).
[16] M. Glerup, O. F. Nielsen, and F. W. Poulsen, J. Solid State Chem. **160**, 25 (2001).
[17] N. J. Hess, B. D. Begg, S. D. Conradson, D. E. McCready, P. L. Gassman, and W. J. Weber, J. Phys. Chem. B **106**, 4663 (2002); P. Nachimuthu, S. Thevuthasan, V. Shutthanandan, E. M. Adams, W. J. Weber, B. D. Begg, D. W. Lindle, E. M. Gullikson, and R. C. Pereira, J. Appl. Phys. **97**, 033518 (2005).
[18] J. Lian, L. M. Wang, S. X. Wang, J. Chen, L. A. Boatner, and R. C. Ewing, Phys. Rev. Lett. **87**, 145901 (2001).
[19] J. Lian, X. T. Zu, K. V. G. Kutty, J. Chen, L. M. Wang, and R. C. Ewing, Phys. Rev. B **66**, 054108 (2002).
[20] Y. Zhang, V. Shutthanandan, R. Devanathan, S. Thevuthasan, D. E. McCready, J. Young, G. Balakrishnan, D. M. Paul, and W. J. Weber, Nucl. Instrum. Methods Phys. Res. B **218**, 89 (2004).
[21] O. Mishima, L. D. Calvert, and E. Whalley, Nature (London) **310**, 393 (1984).
[22] O. Mishima, L. D. Calvert, and E. Whalley, Nature (London) **314**, 76 (1985).
[23] H. Sankaran, S. K. Sikka, S. M. Sharma, and R. Chidambaram, Phys. Rev. B **38**, 170 (1988).
[24] R. J. Hemley, A. P. Jephcoat, H. K. Mao, L. C. Ming, and M. H. Manghnani, Nature (London) **334**, 52 (1988).
[25] Surinder M. Sharma and S. K. Sikka, Prog. Mater. Sci. **40**, 1 (1996).
[26] F. X. Zhang and S. K. Saxena, Chem. Phys. Lett. **413**, 248 (2005).
[27] F. X. Zhang, B. Manoun, S. K. Saxena, and C. S. Zha, Appl. Phys. Lett. **86**, 181906 (2005).
[28] S. Saha, D. V. S. Muthu, N. Dragoe, R. Suryanarayanan, G. Dhalenne, A. Revcolevschi, Nandini Garg, A. K. Mishra, S. M. Sharma, and A. K. Sood, Solid State Phys. **50**, 97 (2005).
[29] F. X. Zhang, J. Lian, U. Becker, R. C. Ewing, Jingzhu Hu, and S. K. Saxena, Phys. Rev. B **76**, 214104 (2007).
[30] A. Apetrei, I. Mirebeau, I. Goncharenko, and W. A. Crichton, J. Phys.: Condens. Matter **19**, 376208 (2007).
[31] R. S. Kumar, A. L. Cornelius, M. F. Nicol, K. C. Kam, A. K. Cheetham, and J. S. Gardner, Appl. Phys. Lett. **88**, 031903 (2006).
[32] F. X. Zhang, J. Lian, U. Becker, R. C. Ewing, L. M. Wang, L. A. Boatner, Jingzhu Hu, and S. K. Saxena, Phys. Rev. B **74**, 174116 (2006).
[33] A. Dewaele, P. Loubeyre, and M. Mezouar, Phys. Rev. B **70**,

094112 (2004).
[34] A. P. Hammersely, S. O. Svensson, M. Hanfland, A. N. Fitch, and D. Hausermann, High Press. Res. **14**, 235 (1996).
[35] A. C. Larson and R. B. von Dreele, *GSAS: General Structure Analysis System*, Los Alamos National Laboratory report LAUR, 86-748 (1994).
[36] R. A. Forman, G. J. Piermarini, J. D. Barnett, and S. Block, Science **176**, 284 (1972).
[37] F. Birch, J. Geophys. Res. **83**, 1257 (1978).
[38] R. Angel (www.crystal.vt.edu/crystal/software.html).
[39] Nandini Garg, K. K. Pandey, Vinod Panchal, V Grover, A. K. Tyagi, and S. M. Sharma, in *Proceedings of DAE Solid State Physics Symposium*, edited by V. K. Aswal, K. G. Bhushan, and J. V. Yakhmi (Times prints, Mumbai, 2005), Vol. 50, p. 109.
[40] W. R. Panero, L. P. Stixrude, and R. C. Ewing, Phys. Rev. B **70**, 054110 (2004).
[41] M. Marques, M. Florez, J. M. Recio, L. Gerward, and J. S. Olsen, Phys. Rev. B **74**, 014104 (2006).
[42] W. Kraus and G. Nolze, J. Appl. Crystallogr. **29**, 301 (1996).
[43] J. M. Leger, A. Atouf, P. E. Tomaszewski, and A. S. Pereira, Phys. Rev. B **48**, 93 (1993).
[44] Since the gasket in the diamond anvil cell shrinks at high pressures, the weight fraction of the tungsten gasket increases with pressure. It was observed that the weight fraction of the tungsten gasket increased from 18.8% (at 18 GPa) to 22.1% (at 30 GPa). This increase in weight fraction of the gasket material will also bring about a corresponding decrease in the weight fraction of the sample peaks.
[45] F. W. Poulsen, M. Glerup, and P. Holtappels, Solid State Ionics **135**, 595 (2000).
[46] M. T. Vandenborre, E. Husson, J. P. Chatry, and D. Michel, J. Raman Spectrosc. **14**, 63 (1983).
[47] M. Glerup *et al.* (Ref. 16) observed that increase in concentration of the dopant atoms leads to the broadening of all the Raman modes along with a reduction in the intensities of the A_{1g}/F_{2g} modes.
[48] A. Jayaraman, S. Y. Wang, S. K. Sharma, and L. C. Ming, Phys. Rev. B **48**, 9205 (1993).
[49] H. Arashi, T. Yagi, S. Akimoto, and Y. Kudoh, Phys. Rev. B **41**, 4309 (1990).
[50] J. P. Perdew, K. Burke, and Y. Wang, Phys. Rev. B **54**, 16533 (1996); J. P. Perdew, K. Burke, and M. Ernzerhof, Phys. Rev. Lett. **77**, 3865 (1996).
[51] P. E. Blöchl, Phys. Rev. B **50**, 17953 (1994).
[52] G. Kresse and D. Joubert, Phys. Rev. B **59**, 1758 (1999).
[53] G. Kresse and J. Hafner, Phys. Rev. B **47**, R558 (1993).
[54] G. Kresse and J. Furthmüller, Phys. Rev. B **54**, 11169 (1996).
[55] F. D. Murnaghan, Proc. Natl. Acad. Sci. U.S.A. **50**, 667 (1944).
[56] Andrej Grzechnik, Wison A. Crichton, Pierre Bouvier, Vladimir Dmitriev, Hans-peter Weber, and Jean-Yves Gesland, J. Phys.: Condens. Matter **16**, 7779 (2004).
[57] T. Sakuntala, A. K. Arora, V. Sivasubramanian, R. Rao, S. Kalavathi, and S. K. Deb, Phys. Rev. B **75**, 174119 (2007).